Polymer Journal, Vol. 26, No. 8, pp 880—894 (1994)

Phase Equilibria in Mixtures of Thermotropic Small Molecular Liquid Crystals and Flexible Polymers

Yuliang YANG,* Jianming LU, Hongdong ZHANG, and Tongyin YU

Department of Macromolecular Science, Fudan University, Shanghai 200433, China

(Received November 5, 1993)

ABSTRACT: Lebwohl–Lasher nematogenic model and Flory–Huggins theory of mixtures have been combined to describe the phase equilibria in mixtures of thermotropic small molecular liquid crystals and flexible polymers. Monte Carlo simulations on the same model have also been carried out in order to confirm the theoretical predictions. A comparison between theory and Monte Carlo simulation gives very good agreement. The findings include a widening of the nematic (N)/isotropic (I) two phase region with increasing polymer chain length and the isotropic force between polymer subunit and nematogen, exclusion of the polymer coils from the nematic phase and the appearance of an I/I biphasic region when the isotropic interaction exceeds the critical Flory–Huggins interaction parameter χ_c. A comparison with a real experimental system is also made and the agreement is quite good considering the simplicity of the theoretical model. A discrepancy between theory and experiment is imputed to the existence of an anisotropic interaction between polymer subunit and nematogen according to the existing ^{2}H NMR results, which has not been taken into account in the present stage of theoretical approach. All of these findings are in accord with the present model and lend support to the general validity of Flory–Huggins treatment of mixtures and the Lebwohl–Lasher model for the thermotropic nematic behavior.

KEY WORDS Liquid Crystal / Flexible Polymer / Statistical Thermodynamics / Phase Equilibrium / Lattice Model / Monte Carlo Simulation /

Thin films composed of small molecular liquid crystalline micro-droplets dispersed in solid polymeric matrices are promising material for electro-optic applications, including information displays and privacy windows.[1-4] These materials are formed by incorporation of small molecular liquid crystals in a cross-linked epoxy binder or in a UV cured polymer matrix.[4-6] This kind of polymer dispersed liquid crystalline (PDLC) material is also formed using thermoplastics which offer a great variety of usable polymers, methods of forming the PDLC materials, and techniques of forming films. In this case, one wants to know the boundaries of various phases, isotropic and nematic, and their transitions depend on the properties of the polymers and small molecular liquid crystals, such as the polymerization indices of polymer and the interaction between polymer and liquid crystalline molecules, etc. Therefore, it stimulates many theoretical and experimental studies on the mixtures of thermotropic small molecular liquid crystals and polymers.[7-9] The present work is also directly motivated by the technical importance of this understanding.

Many statistical theories of the nematic phase have been presented. Among the best known are those of Onsager,[10] Maier and Saupe,[11,12] and Flory.[13] The Onsager treatment has proven successful in the description of rigid molecules with high aspect ratio which display lyotropic behavior, while the Maier–Saupe treatment has found applications to

* To whom correspondence should be addressed.

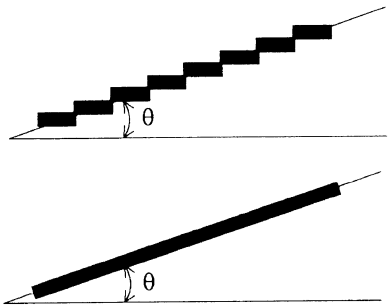

Figure 1. The rod with an angle of inclination from the local domain axis θ is represented as discretized steps in order to fit into the lattice in Flory's approximation.

molecules with lower aspect ratio displaying thermotropic behavior.[14] The extension of the original Flory lattice model for rod-like molecules to a variety of mixtures including the binary mixtures of random polymer coils and nematogens has been made by Ballauff.[15] Comparison between the theory without the isotropic energetic term and experimental data for a relatively large range of polymer molecular weight has been made and found to give very good agreement for polymers with sufficiently high molecular weight.[16] However, in Flory's treatment, the rod with an angle of inclination from the local domain axis θ has to be broken and the angle of rotation about the domain axis should be in discretized steps in order to fit into the lattice, *cf.* Figure 1. It is not difficult to understand that this kind of discretization will be a bad approximation for short rods (rods with lower aspect ratios) and results in underestimation of the entropy resulting from the orientational distribution of liquid crystals.[17,18]

Furthermore, mixing between liquid crystal and polymer is generally not athermal, even when the temperature is higher than that the nematic to isotropic transition temperature of the liquid crystal which indicates a nonzero isotropic interaction energy.

The aim of the present paper is to develop a simple theory for the mixtures of small molecular liquid crystals and flexible polymers, and to confirm the theory by Monte Carlo simulation. We model the flexible polymer chain as a lattice chain and use the Lebwohl–Lasher lattice nematogen model[19,20] rather than discretization model[15,21] for small molecular liquid crystals. The Lebwohl–Lasher model for the small molecular liquid crystal can be considered as a lattice version of the Maier–Saupe treatment which will be more consistent with the lattice model of flexible chains. Another advantage of the Lebwohl–Lasher model is that it can be easily extended to deal with a surface anchored liquid crystalline system,[22] as well as the interface between small molecular liquid crystals and flexible polymers.[23] Furthermore, the model system is especially suitable for Monte Carlo simulation.[24,25]

The paper is organized as follows. In section of THEORY, we develop a simple theory for mixtures of small molecular liquid crystals and flexible polymers based on the model mentioned above, and phase diagrams are calculated according to the theory. In section of MONTE CARLO SIMULATION, we compare the results of section of THEORY with those of the Monte Carlo simulation obtained for the same model system. In section of COMPARISON WITH REAL SYSTEM, we make the primary comparison between the theoretical calculations and experimental data. Finally, we summarize the results in section of CONCLUSION.

THEORY

The Model

Considering a binary system consisting of a flexible polymer and a rod-like nematogen, the sizes of the polymer subunit and nematogen are assumed to be equal to the size of lattice cell. Therefore, the contour length of the coiled lattice chain is x_p and each nematogen with an angle of inclination from the local domain axis θ occupies only one site. Obviously, this kind of model, as schematically shown in Figure 2, is only suitable for mixtures

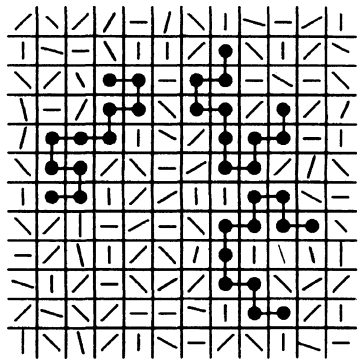

Figure 2. The schematic representation of the model system.

of small molecular liquid crystals and flexible polymers. In spite of the loss of some generalities, we gain the advantages of simplicity and obtain a continuous orientational distribution which we believe important for the calculation of the entropy resulting from the orientational distribution.

In the Lebwohl–Lasher nematogen model,[19,20] a system of uniaxial particles placed at the sites of a cubic lattice interacts through a nearest neighbor pair potential of the form

$$U_{i,j} = -\varepsilon_{ij} P_2(\cos\theta_{ij}) \tag{1}$$

where ε_{ij} is a positive constant, ε_b, for the nearest neighbor particles i and j, $P_2(x)$ is a second Legendre polynomial and θ_{ij} is the angle between the axes of the two molecules. From a formal point of view, eq 1 is a simplified version of the attractive anisotropic interaction put forward by Maier and Saupe.[11,12] Therefore, the Lebwohl–Lasher model can be consisered to be a discretization version of Maier–Saupe model. The potential under the mean field approximation is obtained by standard means.[24] Upon averaging the pair potential in eq 1, we find

$$U = -\varepsilon_b P_2(\cos\theta)\langle P_2\rangle_0 \tag{2}$$

where θ is the angle between the long axes of molecule and the director, and $\langle P_2\rangle_0$ is defined by a self-consistent equation,

$$\langle P_2\rangle_0 = \left\langle \frac{1}{2}(3\cos^2\theta - 1)\right\rangle_0 = \int P_2(\cos\theta) f(\cos\theta)\sin\theta\,\mathrm{d}\theta \tag{3}$$

with the orientational distribution function $f(\cos\theta)$,

$$f(\cos\theta) = \frac{\exp\left\{\left(\frac{z\varepsilon_b}{kT}\right)P_2(\cos\theta)\langle P_2\rangle_0\right\}}{Z_0} \tag{4}$$

where z is the coordination number ($z=6$ for the cubic lattice), and the subscript "0" represents pure liquid crystal; Z_0 is the orientational partition function,

$$Z_0 = \int \exp\left\{\left(\frac{z\varepsilon_b}{kT}\right)P_2(\cos\theta)\langle P_2\rangle_0\right\}\sin\theta\,\mathrm{d}\theta \tag{5}$$

from which the orientational entropy can be calculated through Boltzmann's relation,

$$S = -k\int f\ln(4\pi f)\sin\theta\,\mathrm{d}\theta \tag{6}$$

In a mixture of the flexible lattice chain and the Lebwohl–Lasher nematogen, the z neighboring sites are not all occupied by a Lebwohl–Lasher nematogen. Therefore, the potential energy term in eq 3—5 should be modified when the volume fraction of the Lebwohl–Lasher nematogen is φ_L ($=1-\varphi_P$, with φ_P the volume fraction of polymer segments), *e.g.*, the corresponding partition function is rewritten as

$$Z(\varphi_L) = \int \exp\left\{\left(\frac{z\varepsilon_b}{kT}\right)\varphi_L P_2(\cos\theta)\langle P_2(\varphi_L)\rangle\right\} \times \sin\theta\,\mathrm{d}\theta \tag{7}$$

Free Energy of the Mixture

To calculate the free energy of the mixture, we assume that (i) the interaction between the polymer segments, ε_{PP}, is isotropic, (ii) the interaction between polymer subunit and nematogen, ε_{LP}, is purely isotropic, *i.e.*, the

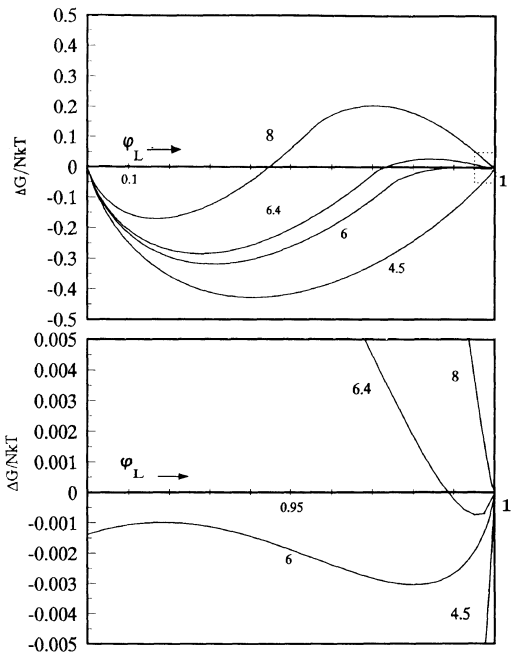

Figure 3. Mixing free energy as a function of volume fraction of nematogens for $x_P=5$ and $\chi_{LP}=0$. The discontinuities and the highly unsymmetry can clearly be seen when $\chi_{LL}>4.541$. The numbers on the curves are the values of χ_{LL}. The lower figure is the enlargement for high concentration of liquid crystal.

polymer chain is completely flexible. We choose the pure liquid crystal at a given temperature as the reference state of liquid crystal. Although the choice of reference state is not important for calculating the phase diagrams, it makes a plot of free energy *vs.* concentration (Figure 3) easier to understand. Following the Flory–Huggins[26] and Lebwohl–Lasher[19,20] theories, the enthalpy of mixing reads,

$$\Delta H_M = n_L\chi_{LP}\varphi_P - \frac{1}{2}n_L\chi_{LL}(\varphi_L\langle P_2(\varphi_L)\rangle^2 - \langle P_2\rangle_0^2) \quad (8)$$

Obviously, the first term of eq 8 represents the isotropic interaction between polymer segments and liquid crystalline molecules which has been ignored in ref 15. The second term in eq 8 denotes the orientational enthalpy change caused by introducing the polymer segments. The apperance of $\langle P_2\rangle_0^2$, the order parameter of reference state of pure liquid crystal, is resulted from the choice of the reference state. Similarly, the entropy of mixing is as follows,

$$\begin{aligned}\Delta S_M &= \Delta S_{conf.} + \Delta S_{orient.} \\ &= -k(n_L \ln \varphi_L + n_P \ln \varphi_P) \\ &\quad - n_L k\{\chi_{LL}\varphi_L\langle P_2(\varphi_L)\rangle^2 \\ &\quad - \ln Z(\varphi_L) + \chi_{LL}\langle P_2\rangle_0^2 - \ln Z_o\} \end{aligned} \quad (9)$$

Where eq 6 has been used to obtain the results of eq 9. Finally, the free energy of mixing can be readily written as,

$$\begin{aligned}\frac{\Delta G_M}{NkT} &= \chi_{LP}\varphi_L\varphi_P \\ &\quad + \frac{1}{2}\chi_{LL}\varphi_L(\varphi_L\langle P_2(\varphi_L)\rangle^2 - \langle P_2\rangle_0^2) \\ &\quad + \varphi_L \ln \varphi_L + \frac{\varphi_P}{x_P}\ln \varphi_P - \varphi_L \ln \frac{Z(\varphi_L)}{Z_o} \end{aligned} \quad (10)$$

where $\chi_{LP}=z\Delta\varepsilon/kT$, $\Delta\varepsilon=\varepsilon_{LP}-\varepsilon_{PP}/2$, and $\chi_{LL}=z\varepsilon_b/kT$ are the interaction parameters for pairs of polymer–nematogen and nematogen–nematogen, respectively; $\langle P_2\rangle$ is the order parameter of the liquid crystals in the mixture which can be calculated by the self-consistent equation, eq 3, with potential energy given in eq 7.

Typical calculated compositional dependencies of the free energy are presented in Figures 3 and 4. The general features are: (i) the free energy curve has a discontinuity where the order parameter $\langle P_2\rangle$ starts to be nonzero, *i.e.*, $z\varepsilon_b\varphi_L/kT>4.541$; (ii) the free energy curves are highly unsymmetry when $\langle P_2\rangle\neq 0$, which is the indication of low solubility of flexible chain in the ordered solvents.

Given the free energy of eq 10, the chemical potentials of polymer and liquid crystal can be obtained by partial differentiation with respect to the numbers of nematogens and polymer molecules n_L and n_p, leading to

$$\frac{\Delta\mu_L}{NkT} = \chi_{LP}\varphi_P^2$$

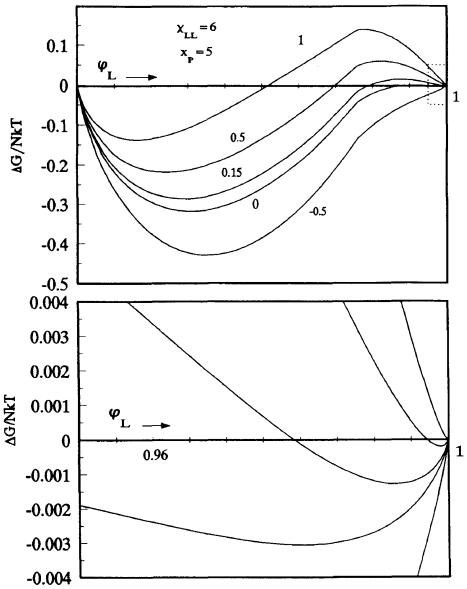

Figure 4. The isotropic potential dependence of the free energy for $\chi_{LL}=6$ and $x_P=5$. The numbers in the figure are the values of χ_{LP}. It is clear that I/N biphasic region is widened when χ_{LP} has larger positive value. The lower figure is the enlargment for high concentration of liquid crystal.

$$+\frac{1}{2}\chi_{LL}(\varphi_L^2\langle P_2(\varphi_L)\rangle^2-\langle P_2\rangle_0^2)$$

$$+\ln\varphi_L+\left(1-\frac{1}{x_P}\right)\varphi_P-\ln\frac{Z(\varphi_L)}{Z_o} \qquad (11)$$

and

$$\frac{\Delta\mu_P}{x_P NkT}=\chi_{LP}\varphi_L^2+\frac{1}{2}\chi_{LL}\varphi_L^2\langle P_2\rangle^2+\frac{1}{x_P}\ln\varphi_P$$

$$+\left(\frac{1}{x_P}-1\right)\varphi_L \qquad (12)$$

for the reduced chemical potentials of the respective compounds at orientational equilibrium.

The calculated chemical potentials of the nematogen and polymers *versus* the volume fraction of polymer segments φ_P are shown in Figure 5. It is not surprising that the chemical potentials have sudden jumps at the nematic to isotropic transition.

The chemical potentials for the isotropic

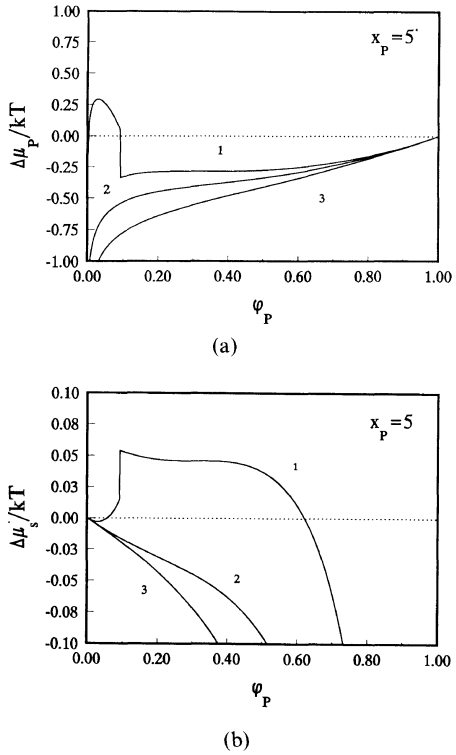

Figure 5. The composition dependence of the chemical potentials for polymer (a) and nematogen (b). (1: $\chi_{LP}=1.05$, $\chi_{LL}=5$; 2: $\chi_{LP}=0.8$, $\chi_{LL}=0$; 3: $\chi_{LP}=0.5$, $\chi_{LL}=0$).

phase of the two components are obtained by setting $\langle P_2\rangle=0$:

$$\frac{\Delta\mu_L}{NkT}=\chi_{LP}\varphi_P^2+\ln\varphi_L+\left(1-\frac{1}{x_P}\right)\varphi_P$$

$$-\frac{1}{2}\chi_{LL}\langle P_2\rangle_0^2+\ln Z_o \qquad (13)$$

and

$$\frac{\Delta\mu_P}{x_P NkT}=\chi_{LP}\varphi_L^2+\frac{1}{x_P}\ln\varphi_P+\left(\frac{1}{x_P}-1\right)\varphi_L \qquad (14)$$

which are the same as the standard Flory–Huggins model.

Phase Diagrams

We have three types of biphasic equilibria, isotropic/isotropic (I/I), isotropic/nematic ($I/$

N) and nematic/nematic (N/N). The requirement for these biphasic equilibria is $\Delta\mu_1=\Delta\mu_2$ for all components present in the system, with the chemical potentials given by eq 11—14. Once x_P, χ_{LP}, and χ_{LL} are known, the equilibrium conditions may be solved numerically from the following equations,

$$\chi_{LP}(\varphi_{L1}^2-\varphi_{L2}^2)-2\chi_{LP}(\varphi_{L1}-\varphi_{L2})+\ln\frac{\varphi_{L1}}{\varphi_{L2}}+\left(\frac{1}{x_P}-1\right)(\varphi_{L1}-\varphi_{L2})+\frac{1}{2}\chi_{LL}\langle P_2(\varphi_{L1})\rangle^2\varphi_{L1}^2-\ln\int_0^1\exp[\chi_{LL}\varphi_{L1}P_2(x)\langle P_2(\varphi_{L1})\rangle]dx=0 \quad (15)$$

and

$$\chi_{LP}(\varphi_{L1}^2-\varphi_{L2}^2)+\frac{1}{x_P}\ln\frac{1-\varphi_{L1}}{1-\varphi_{L2}}+\left(\frac{1}{x_P}-1\right)(\varphi_{L1}-\varphi_{L2})+\frac{1}{2}\chi_{LL}\varphi_{L1}^2\langle P_2(\varphi_{L1})\rangle^2=0 \quad (16)$$

where the relations,

$$\varphi_{L1}+\varphi_{P1}=1\,,\quad \varphi_{L2}+\varphi_{P2}=1 \quad (17)$$

have been used. Equations 15 and 16 include the situations of isotropic/isotropic (I/I) and isotropic/nematic (I/N). The I/I biphasic equilibrium condition is obtained when the equilibrium value of $\langle P_2\rangle$ equals to zero and the isotropic interaction parameter exceeds the critical value χ_c. Equations 10, 15, and 16 are reduced to the situation of monomer and nematogen mixture considered by Hashima *et al.*,[27] when $x_P=1$.

For the monomer/nematogen mixture, eq 15 and 16 can be solved analytically.[27] However, the phase equilibrium condition for the mixture of polymer and nematogen can only be solved numerically as follows: A provisional value of φ_{L1} serves for the numerical evaluation of $Z(\varphi_{L1})$ and the equilibrium value of $\langle P_2(\varphi_{L1})\rangle$ (eq 7 and 3) which are substituted into eq 16 to evaluate φ_{L2}. The calculation is repeated by varying φ_{L1} until self-consistency is achieved. For large x_P, the nematogen-rich phase tends to complete exclude of the flexible random coil. This leads to a numerical difficulty for higher x_P values. This difficulty was overcome through the use of higher digital precision, and approximate solutions can be obtained by setting $\varphi_{L1}<1$ when $\varphi_{P1}<10^{-16}$ for $x_P>40$.

Figure 6 shows the effect of the isotropic interaction energy between polymer and nematogen on the phase behavior. As expected, a negative interaction parameter narrows the biphasic region while a positive value widens this region. The upper phase boundary becomes more severely curved for a positive value of isotropic interaction parameter. As the interaction parameter $z\Delta\varepsilon/kT=\chi_{LP}$ is further increased, *i.e.*, $\chi_{LP}>\chi_c$ ($=1.045$ for $x_P=5$), we can see an I/I biphasic area together with a large I/N biphasic region, Figure 6d. Figure 7 shows the effect of chain length on the lower phase boundary line. We can see that the nematic phase region decreases with increasing the polymer chain length.

MONTE CARLO SIMULATION

We should note that the theoretical results given in Section of THEORY are obtained under the meanfield approximation both for the polymer chain and the nematogen which is inherent in Flory–Huggins model and Maier–Saupe potential. Therefore, the general validity of the meanfield approximation for our system is better to be confirmed by the Monte Carlo simulation for the same model without meanfield approximation under the same microscopic interaction parameter $\varepsilon_b^*=\varepsilon_b/kT$ and $\Delta\varepsilon^*=\Delta\varepsilon/kT$. The comparison between theoretical results and the real system by fitting

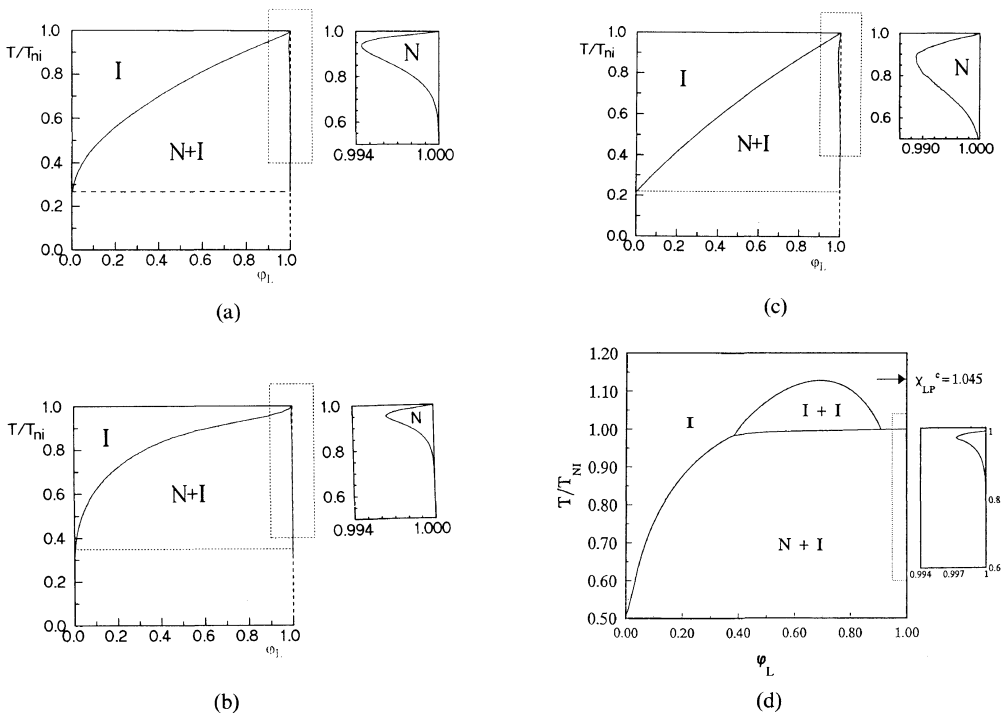

Figure 6. Phase diagrams for nematogen and polymer coil demonstrating the effect of the isotropic interaction parameter $\Delta\varepsilon$. As discussed in the text, a negative interaction parameter narrows the biphasic region (c) while a positive value widens this region (b). When χ_{LP} exceeds the critical value ($=1.045$, for $x_P=5$), I/I demixing occurs prior to I/N demixing (d). The corresponding parameters are: (a) $x_P=5$, $\Delta\varepsilon=0$; (b) $x_P=5$, $\Delta\varepsilon/\varepsilon_b=0.15$; (c) $x_P=5$, $\Delta\varepsilon/\varepsilon_b=-0.15$; (d) $x_P=5$, $\Delta\varepsilon/\varepsilon_b=0.26$, respectively.

the phenomenological Flory–Huggins interaction parameter χ_{LP} and χ_{LL} will be given in Section of COMPARISON WITH REAL SYSTEM.

The Simulation Procedure

The model used for the Monte Carlo simulation is the same as that depicted in Figure 2. The simulation is done in a $10\times10\times10$ cubic lattice with periodic boundary condition as a Monte Carlo unit cell. To simulate the φ_L in the polymer-rich phase, simulations are carried on in a $10\times10\times55$ lattice with the periodic boundary condition in x and y directions. In z direction, there are two impenetrable walls located at z equals to 0 and 56, respectively. Besides the φ_L in polymer-rich phase, the results obtained include the interfacial properties such as concentration profile, surface tension and layer dependence of the order parameters, which will be presented in a future publication.[23] In the unit cell, there are n_P cubic lattice model chains of length x_P and n_P is properly adjusted to fit the desired volume fraction of polymer segments, φ_P. The rest of lattices ($\varphi_L=1-\varphi_P$) are filled with model

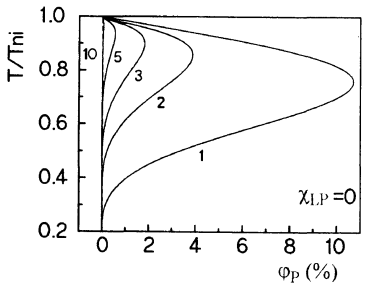

Figure 7. Polymer chain length x_P dependences of the nematicus line. The nematic phase region decreases with increasing the chain length.

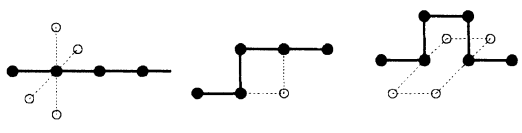

Figure 8. Micro-relaxation modes used in Mote Carlo simulation of cubic lattice chain system. (a) single-bond motion; (b) two-bond motion; and (c) three-bond motion.

nematogens whose orientations are described by their directional cosines. The micro-relaxation modes of polymer chain include the conventional single-bond move for the chain ends, two-bond and three-bond moves for the inner chain segments,[28] which are depicted in Figure 8. The orientation of Lebwohl–Lasher nematogen is sampled by the algorithm described in ref 20. The pair potential of nematogens is given by eq 1 with single parameter ε_b, and the interaction between polymer segment and nematogen is purely isotropic and measured by a single energetic parameter $\Delta\varepsilon$. The simulation procedure can be summarized as following steps:

Step 1. Randomly choose a lattice site;

Step 2. If the chosen lattice is occupied by a nematogen, a new orientation of the nematogen is generated by using the random unit vector which is uniformly distributed on the surface of unit sphere. The energy difference due to the change of orientation, $\Delta\varepsilon_{orient}$, is calculated and the acceptability of the new orientation is determined by use of the Metropolis sampling rule,[29] *i.e.*, the new orientation is accepted when a generated random number $r \in (0, 1)$ satisfies $r \leq e^{-\Delta\varepsilon_{orient.}/kT}$. Here, we should note that even if the new orientation is not accepted, the original state should be counted once again in order to avoid the biase. Then return to Step 1.

If the chosen lattice site is occupied by a chain segment and the local environment (intrachain and interchain) allows for certain micro-relaxation mode, Figure 8, the segments related to certain micro-relaxation mode exchange their positions with the neighboring nematogens while the orientations of these nematogens keep unchanged. The local energy difference due to the exchange of positions is calculated and used for the Metropolis sampling. Whether the move is accepted or not, the simulation continues by turning back to Step 1.

If the chosen segment is not movable, the original state is kept and used once more for calculating the averages. Then return to Step 1.

Step 3. The properties of the system, such as $\langle P_2 \rangle$, are calculated according to the procedure described in next subsection and averaged for each Monte Carlo Cycle ($10 \times 10 \times 10$ times of trial moves).

In every simulation a minimum of 3.0×10^5 cycles are used for equilibrium and thus rejected when calculating averages. The sample size for calculating the averages is larger than 25000 cycles.

It is worth of noting that a much better coarse-grained lattice chain model and Monte Carlo algorithm, four-site model and bond-fluctuation algorithm, have been proposed by Carmesin and Kremer[30] and deeply studied by Baschnagel and Binder *et al.*[31,32] The reason of using the widely used cubic lattice model and relative algorithm is to gain the simplicity.

Calculation of the Order Parameter

There is no external field in our simulation, thus the director of the model system is fluctuating during the simulation and this causes some difficulties for calculating the order parameter $\langle P_2(\varphi_L) \rangle$. Possibly, the simplest way of calculating $\langle P_2(\varphi_L) \rangle$ is the use of order matrix,[33,34]

$$\langle Q \rangle = \begin{bmatrix} \langle x_i^2 \rangle & \langle x_i y_i \rangle & \langle x_i z_i \rangle \\ \langle y_i x_i \rangle & \langle y_i^2 \rangle & \langle y_i z_i \rangle \\ \langle z_i x_i \rangle & \langle z_i y_i \rangle & \langle z_i^2 \rangle \end{bmatrix} \quad (18)$$

where x_i, y_i, and z_i are the directional cosines of i-th nematogen in the lab frame and $\langle \cdots \rangle$ denotes the ensemble average. Three values λ_1, λ_2, and λ_3 obtained by diagonalizing matrix

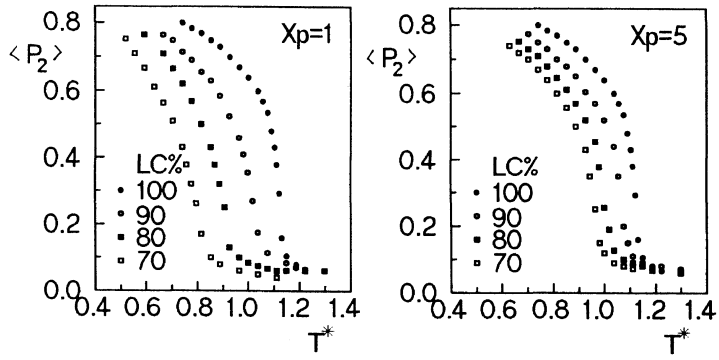

Figure 9. Monte Carlo results of the temperature dependence of the order parameter. The volume fraction of nematogens are shown in the figures. The isotropic interaction energy $\Delta\varepsilon$ has been assigned to be zero in the simulation.

$\langle Q \rangle$ satisfy the relation,

$$\begin{cases} \lambda_1+\lambda_2+\lambda_3=1 \\ \lambda_2=\lambda_3\,, \quad \lambda_1=\lambda_{\max}=\max(\lambda_1, \lambda_2, \lambda_3) \end{cases} \tag{19}$$

The order parameter P_2 is evaluated by using the following equation,

$$\bar{P}_2=\frac{1}{2}(3\lambda_{\max}-1) \tag{20}$$

and then averaged over Monte Carlo Cycles to obtain $\langle P_2 \rangle$. $P(P_2)$, the distribution of P_2, is easily obtained by proper statistics.

We must mention that the director of the system is loose defined for the disordered state. Therefore, the order matrix method can not be used for the disordered system. Practically, it will give nonzero order parameter, $\langle P_2 \rangle$, even if the system is exactly isotropic.[25,34] However, this will not change any conclusion in this simulation. The detailed discussions can be found in ref 35. In any case, eq 20 does give the proper description of the ordered state and the N/I transition.

The N/I transition temperatures are determined by differentiating the spline fitted curve of Monte Carlo simulated data of $\langle P_2 \rangle$ *vs.* T^* as shown in Figure 9. Simulation for the pure Lebwohl–Lasher nematogen system gives the reduced N/I transition temperature $T^*_{\rm NI}=kT_{\rm NI}/\varepsilon_{\rm b}=1.116)\pm 0.005$.[24,25] The mean-field calculation results in higher $T^*_{\rm NI}$ ($=1.321$) due to the neglect of fluctuations.[24] Luckhurst[24] suggested that the scaled dimensionless temperature, T^* ($=T/T_{\rm NI}$), should be used for the comparison between the meanfield calculation and Monte Carlo data or experimental data. This suggestion is followed in this paper.

Results and Comparison between Theory and Simulation

Figure 10 shows the distribution of the order parameter in the vicinity of N/I transition temperature ($T^*_{\rm NI}=1.0836$ for $x_{\rm P}=10$ and $\varphi_{\rm P}=0.10$). The bimodal character of the distribution reveals that the N/I transition is first order even in the mixture.[25] Snapshot pictures of the model system at different temperatures are given in Figure 11, and the aggregation of the polymer chains due to the exclusion of polymer coil from ordered liquid crystalline phase can be clearly observed.

Figure 12 shows the effect of chain length on the upper phase boundary for the model system where isotropic interaction potential $\Delta\varepsilon$ is taken to be zero. The agreement between the meanfield calculations and Monte Carlo data is relatively good. It is shown that the biphasic region widens with increasing chain length, $x_{\rm P}$. The effect of the isotropic potential on the upper critical phase boundary is shown in Figure 13. The magnitudes of $\Delta\varepsilon/\varepsilon_{\rm b}$ used in

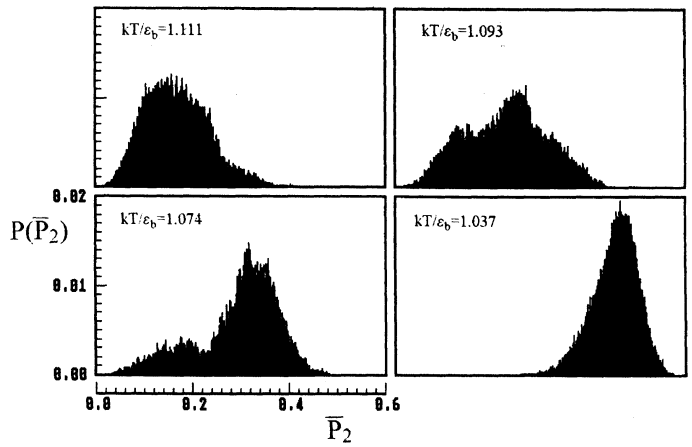

Figure 10. The distribution of the order parameter in the vicinity of the N/I transition temperature ($T^*_{NI}=1.0836$, $x_P=10$, $\varphi_L=0.9$ and $\Delta\varepsilon=0$). The sample size for the statistics is 25000. The bimodal distribution reveals that the N/I transition is first order.

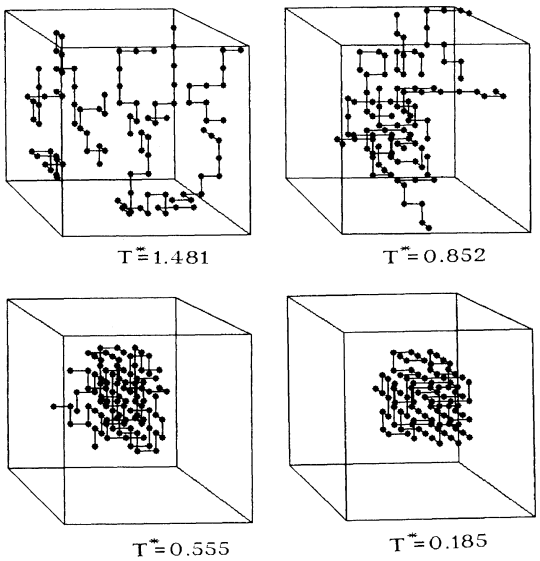

Figure 11. Snapshot pictures for the mixture of polymer and nematogen at different reduced temperatures T^* ($=T/T_{NI}$). For clarity, the nematogens are not shown in the figure. The simulation parameters are the same as those in Figure 8.

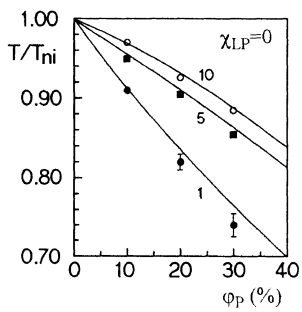

Figure 12. Comparison between Monte Carlo data and mean-field calculations for the upper phase boundary line changes with increasing the chain length. The numbers in the figure are the values of x_P. Symbols are Monte Carlo data and lines are mean-field calculations.

these calculations and simulations are -0.15 and 0.15. Under these conditions there is no possibility of I/I demixing prior to I/N demixing. Obviously, the meanfield calculations agree with the Monte Carlo data fairly well. Similar behavior is also obtained by Dorgan's calculation[16] using Ballauff's theory.[15] Actually, this behavior already reveals that the isotropic potential contribution to the free energy is important. Trail calculations show that this is also true for very large x_P. Therefore, the statement given in ref 15 that for increasing x_P the free energy is mainly determined by its entropic part is not consistent with our findings and Dorgan's calculation.[16]

As predicted by theory, the polymer chains is almost completely excluded by the ordered nematic phase for a longer chain, thus φ_P in the nematogen-rich phase can not be obtained

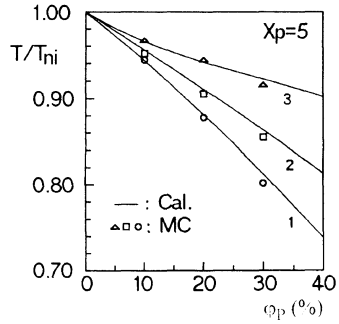

Figure 13. The effect of the isotropic potential energy on the upper phase boundary line. The symbols are the Monte Carlo data; (△) $\Delta\varepsilon/\varepsilon_b=-0.15$; (□) $\Delta\varepsilon/\varepsilon_b=0$; (○) $\Delta\varepsilon/\varepsilon_b=0.15$. The lines are corresponding mean-field calculations.

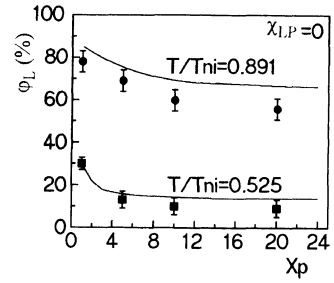

Figure 14. The chain length dependence of nematogen volume fraction in the polymer-rich phase. The symbols are the Monte Carlo data and the lines are the mean-field calculations.

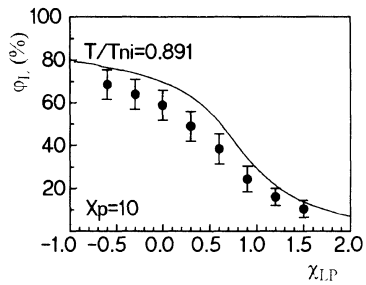

Figure 15. The effect of isotropic interaction parameter on the volume fraction of nematogen in the polymer-rich phase. The symbols are the Monte Carlo data and the solid line is the mean-field calculation.

from the Monte Carlo simulation when a finite sized unit cell is used. On the other hand, φ_L in the polymer-rich phase (isotropic) can be obtained from the simulation with two impenetrable walls. Figures 14 and 15 show the chain length, x_P, and the isotropic interaction term χ_{LP} dependencies of φ_L in the polymer-rich phase. The comparison between theory and simulation shows that the theoretical curves are systematically higher than the Monte Carlo results. In any case, the agreement is reasonably good. The discrepancy may result from the finite size effect of the Monte Carlo unit cell.

A rather interesting result is that φ_L in the polymer-rich phase tends quickly to become constant with increasing x_P, as predicted both by theory and simulation. Therefore, φ_L in polymer-rich phase is more sensitive to the temperature. This is technically quite important in the preparation of a PDLC film, where φ_L in the polymer-rich phase affects the refractive index of the matrix.

COMPARISON WITH REAL SYSTEM

Now we turn to the comparison of model predictions with actually observed phase behavior. To compare with the experimental data, we first need to define a reduced anisotropic interaction potential, U_L, through the N/I transition temperature of pure liquid crystal, T_{NI},

$$\frac{z\varepsilon_b}{kT_{NI}}=\frac{U_L}{T_{NI}}=4.541 \tag{21}$$

For 4-(4-ethoxybenzylidine)-4-butylaniline (EBBA) ($T_{NI}=352.26$ K), we obtain $U_L=z\varepsilon_b/k=1599.6$ K. Here we should note that U_L is just a parameter which measures the strength of the interaction resulting from the Van der Waal's force and spatial exclusion and it should be temperature dependent.[36] However, in the present work, U_L is simply considered as a constant and with the same order approximation as Flory–Huggins interaction parameter.[26] Similarly, the isotropic interaction between polymer segment and nematogen is defined by a single parameter U_P

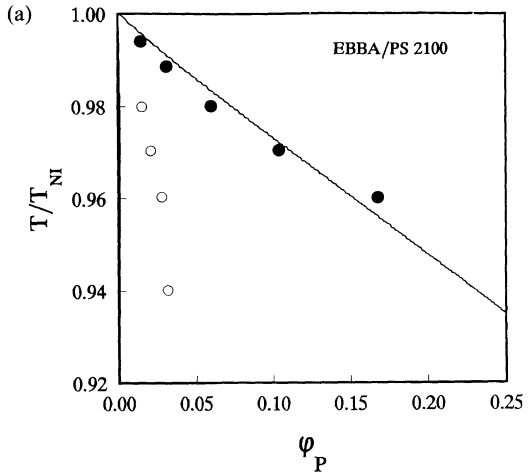

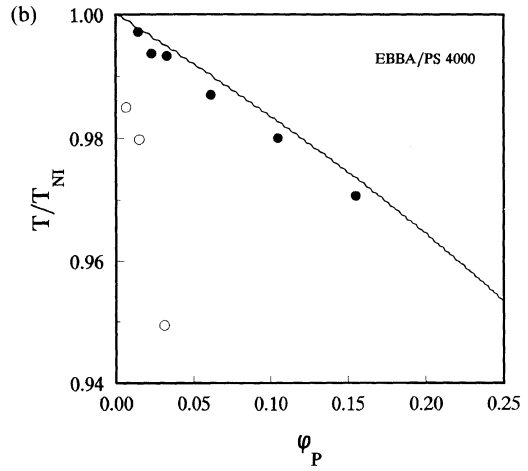

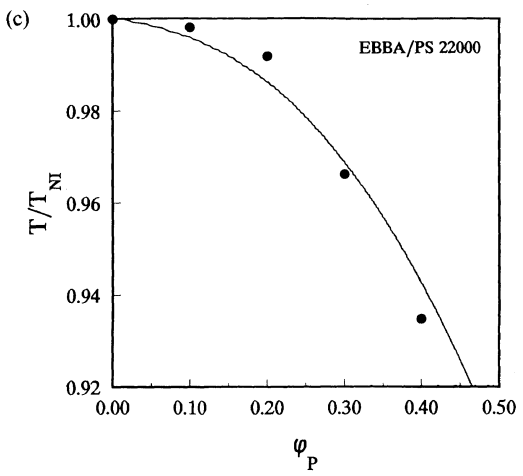

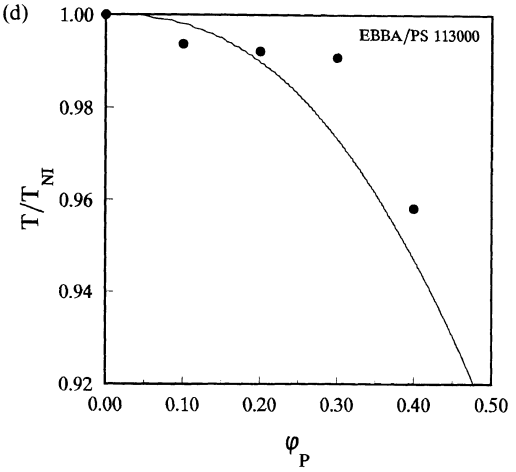

Figure 16. The comparison of the experimental data and the mean-field calculations for the upper phase boundary line. The experimental data are taken from ref 16 and 38 ($\varepsilon_b=266.6$, $\Delta\varepsilon=27.5$). The symbols are the experimental data and the lines are the mean-field calculation. (●) boundary of the isotropic region and the two-phase region; (○) boundary of the nematic region and the two-phase region.

$$\frac{z\Delta\varepsilon}{kT}=\frac{U_P}{T} \tag{22}$$

which we leave as an adjustable parameter in fitting the experimental data.

The number of polymer segments, x_P, is calculated through the data used in ref 15 and 16, *i.e.*,

$$x_P=\frac{x_c}{x_r} \tag{23}$$

where x_r is the aspect ratio of the nematogen ($x_r=3.7$ for EBBA) and x_c is the number of the polymer segments measured by the diameter of the rodlike nematogen. For polystyrene with $M_w=2100$, $x_c=27.8$.[15] Equation 23 is due to the fact that one nematogen occupies one lattice site in the model used in the present work. Although it is not quite sophisticated, the trial calculation demonstrates that the error introduced is nearly inconsequential for the resulting phase diagrams.

In Figure 16, the experimental points were taken from the corresponding graphs in ref 16 and 38 for the mixtures of EBBA and polystyrene. The theoretical calculations take $U_P = 165°K$ which corresponds to a Flory interaction parameter χ_{LP} with an absolute value of approximately 0.47 which is quite reasonable for this system. Therefore, there is no *I*/*I* demixing prior to *I*/*N* demixing as shown experimentally. As is obvious from Figure 16 the agreement is adequate for the upper phase boundary where experimental scatter seems to be more severe. The discrepancy may be caused by the effect of the residual nonuniformity of the polymer sample especially for the sample of high molecular weight. However, the nematic region predicted by the theory is much too small and it can not be seen in Figure 16. The discrepancy of theoretical and measured nematicus line, especially in the case of shorter chains may originate from the difficulties in measuring the nematicus line[38] and the neglect of the volume change when mixing two components. Another possibility is that the phenyl ring of polystyrene molecules takes part in the ordering process which would lead to stabilizing the nematic phase. The present results indicate that this kind of short-range interaction changes considerably while the chain goes from the isotropic to nematic phase. The alignment of the benzene rings on polystyrene chain in the immediate neighborhood of the rodlike nematogen while the globally isotropic coil conformation is kept, which might be quite general in the mixtures of polymers and liquid crystals, is a kind of anisotropic interaction between chain subunit and nematogen. This feature has not been taken into account in the present approach. It is not difficult to imagine that this kind of interaction will tend toward zero when going from the nematic to isotropic phase. Dubault *et al.*[37] have found by ^2H NMR technique that the orientational distribution of the para-axis of the benzene rings on polystyrene chain becomes anisotropic when the solvent undergoes nematic ordering, and the order parameter of this axis has the same temperature dependence as the order parameter of the nematogens although the global coil is not aligned by the nematic field as revealed by neutron scattering experiment. Therefore, the upper phase boundary will not be affected appreciably by a weak anisotropic interaction, but the lower phase boundary (nematicus line) will show a wider nematic phase region caused by stabilizing effect just discussed. However, Dubault *et al.*[37] imputed the results of ^2H NMR to the fact that the nematic order is destroyed by the polymer coil. Obviously, this interpretation does not coincide with the fact of the widened nematic phase region.

Another interesting physical parameter obtained from the experiment data is $\Delta G(trans)$, the free energy necessary to transfer a polymeric chain from the isotropic phase to the nematic phase. From eq 12 and 14, when at a low polymer concentration (*i.e.*, near T_{NI}°) a first order approximation leads to the following relation:

$$\frac{\Delta G(trans)}{kT} = -\ln\frac{\varphi_P^n}{\varphi_P^i} = \frac{1}{2}\chi_{LL}\langle P_2\rangle_0^2 \cdot x_P \tag{24}$$

Where φ_P^i, φ_P^n are the polymer concentrations in the isotropic and nematic phases at the temperature very close to T_{NI}°, respectively; k is the Boltzmann constant. Equation 24 shows that $\Delta G(trans)$ is proportional to the number of chain segments and independent on the istropic interaction between the polymer subunit and nematogen. In fact, the experimental results[38,39] do show that $\Delta G(trans)$ depends more on the size of polymeric solute than on its chemical nature (*cf.* Figure 17). At $T \sim T_{NI}^{\circ}$, χ_{LL} and $\langle P_2\rangle$ have their universal values 4.541 and 0.429. Therefore, the plot of $\Delta G(trans)/kT$ *vs.* x_P will be a straight line with the slope of 0.418. However, the experiment data shown in Figure 17 give the slope of $\sim$0.125 which is much lower than 0.418. The discrepancy is partly due to the improper

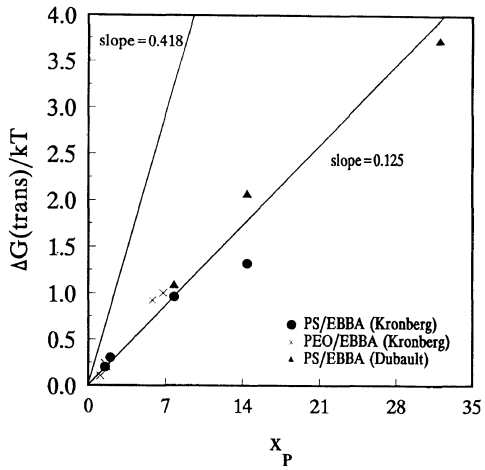

Figure 17. The free energy of transfer *vs.* the chain length. The experimental data are taken from ref 38 and 39. The slope of the fitted line is ~0.125. The theoretical line is calculated from eq 24 the slope is 0.418. (○) is the experimental data for EBBA/PS system from ref 38; (●) is the experimental data for EBBA/PS system from ref 39; and (×) represents the experimental data from ref 39 for the system of EBBA/PEO.

selection of the polymeric subunit volume, as well as the uncertainty of the experiment data. Especially for polymers with high molecular weight, the nematicus line is very steep and the slope of the upper phase boundary line is very low which makes it impossible to determine φ_P^i accurately. Another more important reason is the anisotropic interaction between polymer subunit and nematogen. Brochard *et al.*[40] have shown theoretically that when one component is a polymer with nematogenic side groups, $\Delta G(trans)/kT$ can be written as

$$\frac{\Delta G(trans)}{kT} = -\ln\frac{\varphi_P^n}{\varphi_P^i}$$
$$= \frac{1}{2}(\chi_{LL}\langle P_2\rangle_0^2 - \chi'_{LP}\langle P_2\rangle_0\cdot\langle P_2\rangle_P)x_P \qquad (25)$$

where χ'_{LP} is the anisotropic interaction parameter between nematogenic polymer subunit and nematogen; $\langle P_2\rangle_P$ is the order parameter of nematogenic polymer subunit. Therefore, the lower slope of the experiment data reveals the existence of an anisotropic interaction between polymer subunit and nematogen which coincides with the ^{2}H NMR observations.[37] Certainly, the interpretation should be verified with more experimental and theoretical work.

CONCLUSIONS

We have combined the Lebwohl–Lasher theory of nematic–isotropic transition and the Flory–Huggins theory of mixtures to describe the phase equilibria in mixtures of thermotropic small molecular liquid crystals and flexible polymers. The model is tested against Monte Carlo simulation and found it predicts many of the salient features of the system, which include a widening of the biphasic region with increasing molecular weight of polymer and isotropic interaction parameter between polymer subunit and nematogen, exclusion of the polymer coil from nematic phase. Very good agreement between theory and Monte Carlo simulation is achieved. The comparison with the experimental system is also made and the agreement is also quite good considering the simplicity of the theoretical model. The discrepancy between the theory and experiment is imputed to the existence of anisotropic interaction between polymer subunit and nematogen which has not been taken into account in the present model. this interpretation gains the support from ^{2}H NMR observations[37] and theoretical results[40] for a system in which one component is a polymer with nematogenic side group.

We have shown the importance of the isotropic interaction potential, it can widen the N/I biphasic region and even result in I/I phase separation, in accord with the observation of EBBA/PEO,[39] 7CB/PMMA and 7CB/PS systems.[41] Figure 5 in ref 16 also shows that the calculated N/I biphasic region will be widened considerably when incorporating the isotropic energetic term into Ballauff's theory, even in the case of high molecular weight polymeric

solute. Therefore, the agreement between Ballauff's theory (without the isotropic energetic term) and experiment[15,16] must be regarded as fortuitous. Hence, from these results, it appears that the statement given in ref 15 that for increasing x_P the free energy is mainly determined by its entropic part is questionable. We can conclude that the positive isotropic force is not only important for the apparance of I/I biphasic region, but also promotes the ordering transition by excluding the polymeric coil more strongly from the nematic phase.

This work also lends support to the general validity of the Flory–Huggins treatment of mixtures and the Lebwohl–Lasher model for the thermotropic nematic behavior. A further extension of this work will deal with the interface between phase separated small molecular liquid crystals and the flexible polymers system.

Acknowledgment. Financial supports by National Basic Research Project—Macromolecular Condensed State, NSF of China and FEYUT, SEDC China are gratefully acknowledged.

REFERENCES

1. H. G. Craighead, J. Cheng, and S. Hackwood, *Appl. Phys. Lett.*, **40**, 22 (1982).
2. J. L. Fergason, *SID Digest of Technical Papers*, **16**, 68 (1985).
3. J. W. Doane, N. A. Vaz, B.-G. Wu, and S. Zumer, *Appl. Phys. Lett.*, **48**, 269 (1986).
4. H. D. Zhang, F. M. Li, and Y. Yang, *Functional Polymer (Chinese)*, **4**, 265 (1991).
5. G. P. Montgomery, Jr. and N. A. Vaz, *Appl. Opt.*, **26**, 738 (1987).
6. N. A. Vaz, G. Smith, and G. P. Montgomery, Jr., *Mol. Cryst. Liq. Cryst.*, **146**, 1 (1987).
7. J. L. West, *Mol. Cryst. Liq. Cryst.*, **157**, 427 (1988).
8. G. W. Smith, *Phys. Rev. Lett.*, **70**, 198 (1993).
9. J. Y. Kim and P. Palffy-Muhoray, *Mol. Cryst. Liq. Cryst.*, **203**, 93 (1991).
10. L. Onsager, *Ann. N.Y. Acad. Sci.*, **51**, 627 (1949).
11. W. Maier and A. Saupe, *Z. Naturforsh.*, **14a**, 882 (1959).
12. W. Maier and A. Saupe, *Z. Naturforsh.*, **15a**, 287 (1960).
13. P. J. Flory, *Proc. Royal. Soc., London, Ser. A*, **234**, 73 (1956).
14. S. Chandrasekhar, "*Liquid Crystals*," Cambridge Univ. Press, Cambridge, 1977.
15. M. Ballauff, *Mol. Cryst. Liq. Cryst.*, **136**, 175 (1986).
16. J. R. Dorgan and D. S. Soane, *Mol. Cryst. Liq. Cryst.*, **188**, 129 (1990).
17. P. D. Gujrati, *J. Phys. A: Math. Gen.*, **13**, 437 (1980).
18. W. R. Romanko and S. H. Carr, *Macromolecules*, **21**, 2243 (1988).
19. G. Lasher, *Phys. Rev. A*, **5**, 1350 (1972).
20. P. A. Lebwohl and G. Lasher, *Phys. Rev. A.*, **6**, 426 (1972).
21. J. Sivardiere, *J. Physique*, **41**, 1081 (1980).
22. J. Lu, T. Yu, and Y. Yang, *Science in China*, **36(5)**, 624 (1993).
23. J. Li, Y. Chen, H. Zhang, and Y. Yang *Mol. Cryst. Liq. Cryst*, (accepted).
24. G. R. Luckhurst and G. W. Gray, ed., "The Molecular Physics of Liquid Crystals," Academic Press, London, 1979.
25. H. D. Zhang, J. M. Lu, and Y. Yang, *Chinese J. Comput. Phys.*, **9**, 197 (1992).
26. P. J. Flory, "Principle of Polymer Chemistry," Cornell Univ. Press, Ithaca, New York, 1953.
27. R. Hashim, G. R. Luckhurst, and S. Romano, *Proc. Royal. Soc. London, Ser. A.*, **429**, 323 (1990).
28. H. J. Hilhorst and J. M. Deutch, *J. Chem. Phys.*, **63**, 5153 (1975).
29. N. Metropolis, A. Rosenbluth, M. N. Rosenbluth, A. H. Teller, and E. Teller, *J. Chem. Phys.*, **21**, 1987 (1953).
30. I. Carmesin and K. Kremer, *Macromolecules*, **21**, 2819 (1988).
31. J. Baschnagel, K. Binder, W. Paul, M. Laso, U. W. Suter, L. Batoulis, W. Jilge, and T. Bürger, *J. Chem. Phys.*, **95(8)**, 6014 (1991).
32. H. P. Wittmann, K. Kremer, and K. Binder, *J. Chem. Phys.*, **96(8)**, 6291 (1992).
33. J. Viellard-Baron, *J. Chem. Phys.*, **56**, 4729 (1972); *Mol. Cryst. Liq. Cryst.*, **28**, 809 (1974).
34. I. Ino and K. Ito, *J. Phys. C: Solid State Phys.*, **15**, 4417 (1982).
35. C. Zannoni, *J. Chem. Phys.*, **84**, 424 (1986).
36. P. G. de Gennes, "The Physics of Liquid Crystals," Clarendon, Oxford, **1975**.
37. A. Dubault, A. Ober, M. Veyssie, and B. Cabane, *J. Physique.*, **46**, 1227 (1985).
38. B. Kronberg, I. Bassignana, and D. Patterson, *J. Phys. Chem.*, **82**, 1714 (1978).
39. A. Dubault, C. Casagrande, and M. Veyssie, *Mol. Cryst. Liq. Cryst.*, **72**, 189 (1982).
40. F. Brochard, J. Jouffroy, and P. Levison, *J. Physique.*, **45**, 1125 (1984).
41. W. Ahn, C. Y. Kim, H. Kim, and S. C. Kim, *Macromolecules*, **25**, 5002 (1992).